Hubble Tension: Evidence for Patchwork Quilt Structure of Visible World in World-Universe Cosmology

Vladimir S. Netchitailo
netchitailo.vs@gmail.com

Abstract

The persistent discrepancy between measurements of the Hubble constant H_0 — the fundamental parameter describing the expansion rate of the Universe — has become known as the *Hubble Tension*. Observational determinations of H_0 derived from different methodologies and distance ladders disagree by amounts far exceeding their quoted uncertainties, suggesting that the standard cosmological framework may be incomplete. In this article, we examine the large-scale Macrostructures of the World — Superclusters and Galaxies — and analyze their Origin and Evolution within the Hypersphere World-Universe Cosmology (WUC), a proposed Transformative New Cosmology [1]. Unlike the Big Bang Model, which assumes a practically infinite, homogeneous, and isotropic Universe expanding from an initial singularity, WUC envisions a three-dimensional finite, boundless observable World as a *Patchwork Quilt* composed of $\gtrsim 10^3$ Luminous Superclusters that formed independently in different regions and at different cosmological times. While the Cosmic Medium of the World in WUC remains homogeneous and isotropic, the spatial distribution of Macroobjects is inherently inhomogeneous, anisotropic, and temporally non-simultaneous. We show that this intrinsic Patchwork Quilt structure naturally accounts for the observed variations in H_0, offering a compelling explanation for the Hubble Tension within the WUC framework.

1. Introduction

The workshop *"Tensions between the Early and the Late Universe"* was held at the Kavli Institute for Theoretical Physics on July 15–17, 2019, to assess the growing evidence for discrepancies in key cosmological measurements—most notably the value of the Hubble constant—and to examine recently proposed ideas aimed at resolving this tension. During the workshop, multiple new observational determinations of the Hubble constant were presented using a variety of independent probes, including Cepheid variables, strong-lensing time delays, and others. Importantly, the emerging discrepancies do not appear to depend on any single method, data set, or research group.

In their summary article *"Tensions between the Early and the Late Universe"* [2], L. Verde, T. Treu, and A. G. Riess emphasized that while the standard cosmological model successfully accounts for observations spanning a wide range of epochs—from primordial nucleosynthesis to the present-day accelerated expansion—it is not guaranteed to remain valid as the precision of cosmological measurements continues to improve. Increasingly precise observations from different cosmic eras may eventually strain the model's internal consistency. The growing mismatch between early- and late-Universe determinations of cosmological parameters, particularly the Hubble constant, **may signal the need to extend the standard model and could point toward new physics.**

Appendix 1 summarizes the measurements of the Hubble constant H_0 obtained between 1994 and 2025 [3]. These values vary substantially depending on the methodology used. The disagreement between the measurements—often far exceeding the quoted uncertainties—clearly illustrates the severity of the problem. The averaged values of H_0 span a broad range, from **66.6** to **76.9 km s^{-1} Mpc^{-1}**, with **21** measurements lying between **66.6–68.76 km s^{-1} Mpc^{-1}** and **30** measurements between **69.32–76.9 km s^{-1} Mpc^{-1}**. This persistent

and statistically significant inconsistency is known as the **Hubble tension**. In 2019, A. Mann summarized the situation in the article *"One Number Shows Something Is Fundamentally Wrong with Our Conception of the Universe"* [4], underscoring that the tension represents a major challenge to a Standard Cosmological Model.

2. Macrostructures of the Visible World

The **Laniakea Supercluster** (LSC) is the vast galaxy supercluster that contains the Milky Way (MW) and roughly 100,000 neighboring galaxies (**Figure 1**). It is one of the largest known superclusters, with an estimated binding mass of $\sim 10^{17} M_{\odot}$. Nearby major superclusters include the Shapley, Hercules, Coma, and Perseus–Pisces Superclusters. The distance from Earth to the center of LSC is approximately 250 Mly.

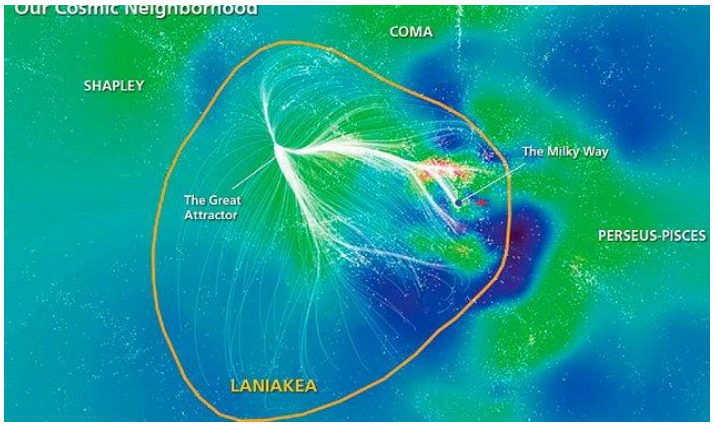

Figure 1. Laniakea Supercluster. Adapted from [5].

A key structural feature of Laniakea is the **Great Attractor**, a massive region acting as a gravitational focal point for the galaxies within LSC. Although not a single object, it represents a dense concentration of galaxies and dark matter located behind the Zone of Avoidance, making direct optical observation difficult. Nevertheless, its gravitational influence is unmistakable!

Key details:

- **LSC**: A vast supercluster of ~100,000 galaxies, including the MW; the name "Laniakea" means "immense heaven" in Hawaiian.
- **Great Attractor**: The dynamical center of LSC, containing a mass of order $10^{16} M_{\odot}$, shaping the motion and flow of galaxies within the supercluster.
- **Our location:** The Milky Way sits near the outskirts of Laniakea, within the Virgo Cluster, and is moving toward the Great Attractor.

The influence of the Great Attractor is inferred from peculiar velocities of galaxies—systematic deviations from a pure Hubble flow. Although most galaxies are redshifted overall (consistent with cosmic expansion), the variations in these redshifts are large and coherent enough to reveal a net flow toward the attractor. These peculiar velocities range from roughly +700 km/s to −700 km/s, depending on the galaxy's angular position relative to the Great Attractor. The attractor itself is moving toward the Shapley Supercluster.

Although the center of Laniakea has a redshift of z = 0.0708, this does not imply that it is receding from the MW. Instead, the **Milky Way is moving within the gravitational potential of the supercluster**. Some galaxies in LSC are moving toward us, while others move away. Their redshifts therefore depend on their location and motion within Laniakea. The situation becomes even more complex for galaxies associated with neighboring superclusters (**Figure 2**). As noted by S. Gupta, more than 8300 blue-shifted galaxies beyond the

Local Group were known by 2009 [6]. The Andromeda Galaxy—the nearest major galaxy—is also blue-shifted. Explaining these observations consistently within standard cosmology remains challenging.

According to WUC, the Hubble parameter should be determined exclusively from the Cosmic Microwave Background (CMB) Radiation, which reflects the properties of the homogeneous and isotropic Cosmic Medium. The value calculated in 2013 [7]:

$$H_0 = 68.73\,\mathrm{km\,s^{-1}\,Mpc^{-1}},$$

is in excellent agreement with the 2021 determination based solely on CMB data (see **Appendix 1**):

$$H_0 = 68.7 \pm 1.3\,\mathrm{km\,s^{-1}\,Mpc^{-1}}.$$

The mass-to-light ratio in the Virgo supercluster is roughly 300 times the Solar ratio, and similar values are found in other superclusters [8]. Already in 1933, F. Zwicky measured the velocity dispersion in the Coma supercluster and derived a ratio of ~500, concluding that dark matter must exceed luminous matter by a large factor [9]. Such high ratios remain fundamental evidence for significant amounts of dark matter in the Universe.

We emphasize that the ~100,000 galaxies within Laniakea are **orbiting the center of the supercluster** (the **Attractor**). They are bound members of LSC and did not originate from a single "initial singularity" in the sense implied by the Standard Model. Neighboring superclusters show analogous structures (**Figure 2**). Together, they indicate that the Visible World is, in fact, a **Patchwork Quilt** of $\gtrsim 10^3$ luminous superclusters.

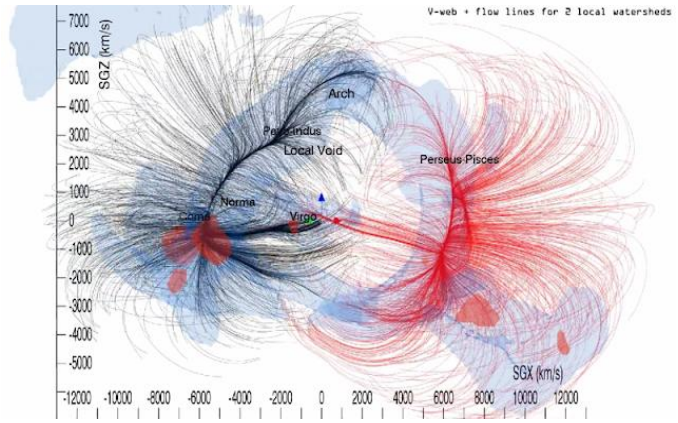

Fig. 2. A representation of structure and flows due to mass within 6,000 km s-1 (80 Mpc). Adapted from [5].

According to R. B. Tully, *et al.*, "*Galaxies congregate in clusters and along filaments, and are missing from large regions referred to as voids. These structures are seen in maps derived from spectroscopic surveys that reveal networks of structure that are interconnected with no clear boundaries"* [5].

P. Wang, *et al.* made a great discovery: "*Most cosmological structures in the universe spin. Although structures in the universe form on a wide variety of scales from small dwarf galaxies to large super clusters, the* ***generation of angular momentum across these scales is poorly understood****. We have investigated the possibility that filaments of galaxies - cylindrical tendrils of matter hundreds of millions of light-years across, are themselves spinning. We have found that these objects too display motion consistent with rotation making them the largest objects known to have angular momentum.* ***These results signify that angular momentum can be generated on unprecedented scales***" [10].

A. Lopez reported about the discovery of "*a giant, almost symmetrical arc of galaxies – the Giant Arc – spanning 3.3 billion light years at a distance of more than 9.2 billion light years away that is* ***difficult to explain***

in current models of the Universe. *This new discovery of the Giant Arc adds to an* ***accumulating set of (cautious) challenges to the Cosmological Principle***. *The growing number of large-scale structures over the size limit of what is considered theoretically viable is becoming harder to ignore.* ***Can the standard model of cosmology account for these huge structures in the Universe as just rare flukes or is there more to it than that?"*** [11].

WUC. These latest observations of the World can be explained in frames of the developed WUC only [1]:

- "*Galaxies* ***do not*** *congregate in clusters and along filaments."* On the contrary, Cosmic Web that is "*networks of structure that are interconnected with no clear boundaries"* is the result of the Explosive Volcanic Rotational Fission of Universe Created Matter (UCM) Cores of neighboring Superclusters.
- *"Generation of angular momentum across these scales"* provide UCM Cores of Superclusters through the Explosive Volcanic Rotational Fission.
- *"Spinning cylindrical tendrils of matter hundreds of millions of light-years across"* are the result of spiral jets of galaxies generated by UCM Cores of Superclusters with internal rotation.
- The Giant Arc is the result of the intersection of the Galaxies' jets generated by the neighboring UCM Cores of Superclusters.
- 13.77 *Gyr* ago, when the Laniakea Supercluster emerged, the estimated number of UCM major Supercluster Cores in the World was around $\sim 10^3$ [1]. It is unlikely that all of them gave birth to Luminous Superclusters at the same cosmological time being far away from each other. The 3D Finite Boundless Visible World presents a Patchwork Quilt of different major Luminous Superclusters, which emerged at different Cosmological times.
- The main conjecture of Big Bang Model (BBM): "*Projecting galaxy trajectories backwards in time means that they converge to the Initial Singularity at t=0 that is an infinite energy density state*" is wrong because all Galaxies are gravitationally bound with their Superclusters (**Figure 1**, **Figure 2**).

3. Explosive Volcanic Rotational Fission Model [12]

3.1. Universe-Created Matter

In our previous articles, we followed the standard paradigm of "Dark Matter," which is not appropriate within the framework of WUC. Instead, WUC posits that the World consists solely of particles of **Ordinary Matter**—protons, electrons, photons, and neutrinos—and a distinct class of particles created by the **Eternal Universe itself**. These particles, called **Universe-Created Particles (UCPs)**, constitute a new type of **Universe-Created Matter (UCM)**.

3.1.1. In 2024, we introduced the term UCPs, which possess the following key characteristics:

- They can be **fermions (UCFs)** or **bosons**.
- Their **rest energies** are given in **Table 1**.
- They interact via the **weak interaction**.
- They undergo **self-annihilation**, similar to Majorana fermions.
- Ordinary particles are produced as **byproducts** of UCPs self-annihilation.

This framework allows an easy conceptual transition from traditional **Dark (D) Matter** to **Universe-Created (UC) Matter** as used in WUC.

3.1.2. Optical Invisibility vs. Multi-wavelength Observability

These Universe-Created particles are "dark" only in the narrow sense that they are **optically invisible**

when observed through telescopes using visible light. However, modern astronomy spans wavelengths from **radio** to **gamma rays**, and in this broader context, UCM is not "dark" at all.

The diversity of non-optical observations supports this view [12]:

- **Cygnus X-1** (1971), the first known X-ray binary, is a persistent bright source of **hard X-rays up to 60 keV**.
- In **2000**, R. Minchin *et a*l. discovered the binary galaxy system **VIRGOHI 21–NGC 4254**, exhibiting strong **21-cm radio emission**.

3.1.3. Two Origins of Radiation in the World

WUC distinguishes the radiation of Ordinary Matter from that of Universe-Created Matter:

1. **Ordinary Matter** radiates electromagnetic waves — from radio to X-rays — through *electrons* outside nuclei. For example, Livermore experiments probed nitrogen gas at X-ray energies up to **8 keV**, the highest ever achieved at an X-ray free-electron laser.
2. **Universe-Created Matter** radiates **gamma rays**, emitted by *nuclei* as a result of **UCPs self-annihilation**. Their rest energies span **eighteen orders of magnitude** (**Table 1**), producing a wide variety of gamma-ray signatures.

3.1.4. Purpose of the Multicomponent UCM System

This multicomponent UCM system was introduced to explain:

- The **diversity of Very High Energy (VHE) gamma-ray sources** observed in the visible World.
- The **diversity of UCM cores** in Macroobjects—Superclusters, Galaxies, and Extra-Solar Systems (ESS)—which in WUC function as **Fermion Compact Objects** and **UCM Reactors**.

Because UCPs carry **no electric charge**, their masses cannot be directly measured through mass spectrometry. They can only be detected **indirectly** via their annihilation signatures.

3.1.5. Observable Signatures of UCP Self-Annihilation

Expected rest energies from UCPs self-annihilation include: **1.3 TeV; 9.6 GeV; 70 MeV; 340 keV; 3.7 keV; 0.2 eV.** These energies appear in:

- the spectra of the **diffuse gamma-ray background**, and
- emissions from various **Macroobjects** throughout the World.

We associate these observed gamma-ray features with the **internal structure** of Macroobjects — their nuclei and shell compositions. Different combinations of UCPs naturally yield a corresponding diversity of gamma-ray lines. Thus, within WUC, the observed richness of Very High Energy gamma-ray sources receives a coherent and natural explanation.

Table 1. Universe-Created Particles**.**

Fermion			Boson		
Particle	**Rest Energy**	**Value**	**Particle**	**Rest Energy**	**Value**
UCF1	$\alpha^{-2}E_0$	1.3149948 TeV	DIRAC	$\alpha^{0}E_0$	70.025252 MeV
UCF2	$\alpha^{-1}E_0$	9.5959804 GeV	ELOP	$2/3\alpha^{1}E_0$	340.66596 keV
UCF3	$\alpha^{2}E_0$	3.7289394 keV	XION	$1/2\,\alpha^{6}E_0$	5.2870895 μeV
UCF4	$\alpha^{4}E_0$	0.19857107 eV			

In this table, the **Basic Energy Unit**

$$E_0 = hc/a = 70.025252 \text{ MeV},$$

where h is the Planck constant, c is a gravitodynamic constant, a is a basic length unit, and α is the dimensionless Rydberg constant [1].

3.2. Macroobject Shell Model

In WUC, the Macrostructures of the World—Superclusters, Galaxies, and Extrasolar Systems (ESS)—contain **nuclei composed of UCFs**, surrounded by **nested shells** made of UCM and Baryonic Matter. These shells are arranged concentrically, *like a Russian doll*. Their structure follows a simple principle:

- **The lighter the particle, the larger the radius and the greater the mass of its shell.**
- **The heaviest particles occupy the innermost shells, the lightest form the outermost layers.**

A proposed **weak interaction among UCPs** maintains the structural integrity of all shells. **Table 2** summarizes the parameters of Macroobject (MO) Cores, modeled as **3D viscous fluid spheres** whose high effective viscosity allows them to behave as solid-state objects.

Table 2. Parameters of Macroobject Cores Composed of Different Fermions (Present Epoch).

Fermion	Fermion Rest Energy, MeV	Macroobject Mass M_{max}, kg	Macroobject Radius R_{min}, m	Macroobject Density ρ_{max}, kgm^{-3}
UCF1	1.3×10^{6}	1.9×10^{30}	8.6×10^{3}	7.2×10^{17}
UCF2	9.6×10^{3}	1.9×10^{30}	8.6×10^{3}	7.2×10^{17}
Electron-Positron	0.51	6.6×10^{36}	2.9×10^{10}	6.3×10^{4}
UCF3	3.7×10^{-3}	1.2×10^{41}	5.4×10^{14}	1.8×10^{-4}
UCF4	2×10^{-7}	4.2×10^{49}	1.9×10^{23}	1.5×10^{-21}

3.2.1. Shell Composition and Macroobject Types

From these calculated parameters, WUC predicts:

- **Cores of stars in Extrasolar Systems (ESS)** consist of **UCF1 and/or UCF2 nuclei**.
- **Cores of Galaxies** are formed by **UCF1/UCF2 nuclei** enveloped by shells of **UCF3** and/or **electron–positron plasma**.
- **Cores of Superclusters** contain **UCF1/UCF2 nuclei**, surrounded by successive shells of **UCF3** and **UCF4**.

Accordingly, **Galactic Cores** are **Supermassive Compact Objects (SMCOs)** composed of UCF1 and/or UCF2, with an outer UCF3 shell. Their **maximum mass**, derived from **Table 2**, is approximately: $6 \times 10^{10} M_{\odot}$. Remarkably, this theoretical limit aligns with observational data for the most massive known dark compact object: the **6.6×10^{10}** $M_{\odot}$ central object in **TON 618** [13].

It is essential to emphasize that **WUC contains no black holes**; instead, such observations correspond to **UCM-based SMCOs**.

3.2.2. Empirical Confirmation of WUC Predictions

The **2020 Nobel Prize in Physics**—awarded to R. Genzel and A. Ghez for the discovery of a supermassive compact object at the center of the Milky Way—provides strong observational support for a key prediction of WUC first stated in 2013:

"*Macroobjects of the World have cores made up of the discussed DM (UCM) particles. Other particles, including DM (UCM) and baryonic matter, form shells surrounding the cores*" [7].

This structure, now supported by precise stellar-orbit measurements, remains a fundamental and distinctive component of the WUC framework [14].

3.3. Angular Momentum

The **Angular Momentum problem** is one of the most critical unresolved issues in the Standard Cosmological Model. Any viable theory of cosmic evolution must explain the origin and conservation of angular momentum across all scales. To the best of our knowledge, **WUC is the only existing cosmological model fully consistent with the Law of Conservation of Angular Momentum**.

To satisfy this requirement, a cosmological model must answer the following fundamental questions:

- How did **Galaxies** and **Extrasolar Systems (ESS)** acquire their substantial orbital and rotational angular momenta?
- How did the **Milky Way (MW)** give birth to numerous ESS at different cosmological times?
- If the MW is approximately as old as the World itself, what is the origin of its enormous orbital and rotational angular momenta? A discussion of the *Beginning of the MW* is required.
- Why is the oldest known star in the MW—**Methuselah**—nearly as old as the Universe?
- The Solar System formed 4.57 Byr ago. What is the origin of its rotational and orbital angular momenta? This requires addressing the *Beginning of the Solar System*.

3.3.1. Rotational Fission as the Source of Angular Momentum

In our view, there is only **one physical mechanism** capable of imparting angular momentum to Macroobjects (MOs): **Rotational Fission of overspinning Prime Objects**, whose equatorial surface velocities exceed their escape velocities.

According to the Fission Model:

- A **Prime Object** transfers part of its *rotational* angular momentum to the *orbital* and *rotational* angular momenta of the objects formed from it.
- Consequently, **the rotational angular momentum of the Prime Object must exceed the total orbital angular momenta of its satellites** [12].

3.3.2. Prime Objects in WUC and the Dark Epoch

Within WUC, **Prime Objects** are **UCM Cores of Superclusters**, which must accumulate enormous angular momenta *before* the birth of the Luminous World. This requires a sufficiently long preparatory phase. We designate this interval as the **Dark Epoch**, and it forms the basis of the New Cosmology in WUC.

- **Dark (Invisible) Epoch** — lasting from the Beginning of the World **14.22 Byr ago** for **0.45 Byr**, when only UCM Macroobjects existed.
- **Luminous Epoch** — beginning **13.77 Byr ago** (for the Laniakea Supercluster) and continuing to the present, during which Luminous Macroobjects emerged through the **Explosive Volcanic Rotational Fission** of Supercluster UCM Cores and through UCPs self-annihilation.

3.3.3. Transfer of Angular Momentum in WUC

- The **UCM Cores of Superclusters** are the primary engines of the Visible World: during the Dark Epoch they accumulated vast rotational angular momenta, which were subsequently transferred to the **UCM Cores of Galaxies** during their Rotational Fission.
- Observationally, the majority of galaxies are **disk galaxies**, strongly suggesting a rotationally driven formation mechanism consistent with Rotational Fission.
- The **UCM Core of the Milky Way** was created **13.77 Byr ago** as a direct result of Rotational Fission of the **Virgo Cluster's** UCM Core.
- **UCM Cores** of ESS, planets, and moons formed through **repeated Rotational Fissions** of Galactic UCM Cores at different cosmological times – e.g.,**4.57 Byr ago** for the Solar System within the MW.

3.3.4. Top–Down Formation of Structure in WUC

In WUC, Macroobjects form in a hierarchical **top–down sequence**:

1. **Superclusters**
2. **Galaxies**
3. **Extrasolar Systems**
4. **Planets**
5. **Moons**

This structure arises naturally from cascading Rotational Fissions of increasingly smaller UCM Cores, propagating the transfer and conservation of angular momentum throughout the World.

3.4. Formation of Macrostructures

3.4.1. Cores of all Macroobjects (MOs) share a common set of fundamental properties:

- **Core–Shell Structure:** The nuclei of all MOs are composed of **Universe-Created Fermions (UCFs)**. These nuclei are surrounded by concentric shells containing **Universe-Created Matter (UCM)** and **Baryonic Matter**.
- **Continuous UCPs Absorption and Matter Production:**
  Universe-Created Particles (UCPs) are continuously absorbed by the cores of all MOs. **Ordinary Matter**, comprising approximately **7.2% of total matter (4.8% in the Cosmic Medium and 2.4% in MOs)**, is produced as a byproduct of **UCPs self-annihilation** and is continuously re-emitted by MO cores. Consequently, MO cores function as **UCM Reactors**, fueled by UCPs. All chemical elements, compositions, and radiative outputs are generated *in situ* through UCPs self-annihilation within UCM cores.
- **Time Evolution of Nuclei and Shells:**
  Both nuclei and shells grow with the **absolute cosmological time τ** according to:
  $$\text{Size} \propto \tau^{1/2}, \quad \text{Mass} \propto \tau^{3/2}, \quad L_{\text{rot}} \propto \tau^{2}.$$
  Growth continues until a **critical stability threshold** is reached, at which point the system undergoes detonation.

3.4.2. Detonation and Satellite Formation

- **Overspinning UCM Cores:**
  At the critical point, **overspinning UCM cores** undergo detonation. This process releases **satellite cores**, together with their **orbital (L_{orb})** and **rotational (L_{rot})** angular momenta.
- **Nature of Detonation:**
  The detonation does **not destroy** the parent core. Instead, it manifests as a **gravitational hyper-flare**, ejecting satellite UCM cores while preserving the integrity of the prime object.
- **Origin of Diversity:**
  The size, mass, composition, and angular momenta ($L_{\text{orb}}, L_{\text{rot}}$) of satellite UCM cores depend on:
  - local density fluctuations at the edge of the prime UCM core, and
  - the cohesion properties of its outer shell.

  This naturally explains the observed **diversity of satellite Macroobjects**.
- **Volcanic Ejection Mechanism:**
  Satellite UCM cores are emitted through localized eruptive regions—**"volcanoes"**—on the surface of prime UCM cores. These eruptions occur **repeatedly**, giving rise to hierarchical structure formation. WUC refers to this detonation process of prime UCM cores as a **Gravitational Burst (GB)**, by analogy with a **Gamma-Ray Burst**.

3.4.3. Repeating Gravitational Bursts

In the WUC framework, **recurrent GBs** arise naturally through the following cycle:

- During each GB, a prime UCM core loses a **small fraction of its mass** but a **large fraction of its rotational angular momentum**.
- After the GB, the core resumes absorbing UCPs:
$$M \propto \tau^{3/2}, L_{\text{rot}} \propto \tau^2,$$
until the next stability threshold is reached and another GB occurs.
- This cyclic process explains why:
  - satellite UCM cores rotate about their own axes, and
  - satellites orbit the UCM cores of their prime objects.

3.4.4. Afterglow Phenomena

- **General Afterglow:**
The **afterglow of a GB** is produced by post-detonation processes within the nuclei and shells of UCM cores.
- **Extrasolar Systems:**
In ESS, the **stellar wind** is the afterglow of a star's UCM core detonation. The core continues to absorb UCPs, increasing its mass ($\propto \tau^{3/2}$), while excess rotational angular momentum is shed through wind particles.
- **Solar System:**
The **solar wind** represents the afterglow of the Solar UCM core detonation **4.57 Byr ago**, continuously forming the **heliosphere (solar bubble)**.
- **Galaxies:**
In galaxies, **galactic winds** are the afterglow of repeated galactic UCM core detonations. In the Milky Way, this process continuously sustains the two **UCM Fermi Bubbles**.

4. Hubble Tension: Explanation within WUC

Observations show that the majority of galaxies in the Universe are **disk galaxies** [15]. For spiral galaxies, the side rotating toward the observer exhibits a slight **blueshift**, while the receding side exhibits a **redshift**. Consequently, a physically meaningful redshift can be defined only for the **galactic center**, not for the galaxy as a whole.

The measured redshift of the **center of the Laniakea Supercluster (LSC)** is $z = 0.0708$. This value does **not** imply that the LSC is moving away from the Milky Way (MW). On the contrary, it indicates that the **MW is moving away from the center of the LSC**. Within LSC, some galaxies move toward the MW while others recede from it (see **Figure 1**). Thus, the observed redshift of any particular galaxy depends strongly on its **location and kinematics relative to the MW**, rather than on a universal recession velocity.

The situation becomes even more complex when galaxies belong to **different superclusters**, which in WUC form at **different cosmological times**. In such cases, redshift is influenced not only by relative motion but also by the **epoch of formation** of the host supercluster.

4.1. Time Dependence of the Hubble Parameter in WUC

In WUC, the Hubble parameter is not a constant but depends explicitly on **cosmological time**:
$$H = \tau^{-1}.$$
This implies that **earlier epochs correspond to larger values of** H.

As a result, the value of the Hubble parameter must be inferred from observables that probe the **Cosmic Medium itself**, rather than from properties of individual Macroobjects. The **Cosmic Microwave Background (CMB) Radiation** uniquely satisfies this requirement, as it reflects the properties of a **homogeneous and isotropic cosmic medium**.

Figure 3 presents recent determinations of H_0 using **CMB data only**, which exhibit strong internal consistency.

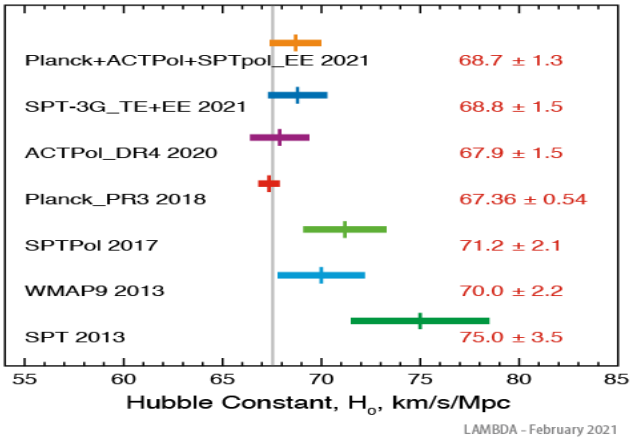

Figure 3. Recent H_0 determinations based exclusively on **CMB** data. Adapted from [16].

4.2. Origin of the Hubble Tension

Within the WUC framework, the Hubble Tension arises naturally due to the following factors:

- All determinations of the Hubble constant are **model-dependent**.
- The available statistics are **insufficient** to justify averaging disparate measurements into a single universal value.
- **Hubble's law**, as used in Standard Cosmology, is valid only within the **Big Bang Model (BBM)**, where all galaxies originate from a single initial singularity—an assumption explicitly rejected by WUC.
- Observational samples include galaxies belonging to **different superclusters**, which formed at **different cosmological times**.
- Since $H = \tau^{-1}$, the value of H must, in principle, be **different for each galaxy**, depending on its distance and corresponding cosmological time.
- Averaging values of H across different methods and objects—as commonly done—has no physical justification in WUC.
- The **only physically meaningful determination of** H is one based on **CMB observations**.

4.3. BBM vs. WUC: Fundamental Differences

The fundamental differences between BBM and WUC may be summarized as follows.

Initial Conditions

- **BBM:**
  Postulates an initial spacetime singularity characterized by infinite energy density and an extremely rapid early expansion (inflation). Within this framework, the three-dimensional universe has no center of expansion.
- **WUC:**
  Proposes that a fluctuation within the Eternal Universe gave rise to a four-dimensional **Nucleus of the**

World, whose extrapolated initial radius equals the fundamental length unit a . The Nucleus expands along the fourth spatial dimension at the speed c , interpreted as a gravitodynamic constant. This expansion produces a uniform stretching of its hyperspherical boundary—the World in WUC—thereby accounting for cosmic expansion without invoking Dark Energy. .

Structure of the World

- **BBM:**
  Assumes an almost infinite universe that is homogeneous and isotropic on large scales, centered conceptually around the initial singularity.
- **WUC:**
  Describes a *Finite Boundless World*—the Hypersphere of the 4D Nucleus, constituting an Absolute Space. The Visible World, which is a 3D Hubble Bubble, is a *Patchwork Quilt* composed of major luminous superclusters ($\gtrsim 10^3$) that emerged in different regions of the World at different cosmological times.

Medium of the World

- **BBM:**
  Commonly implies a vacuum-like state for the early universe, with matter and radiation emerging later.
- **WUC:**
  Introduces a **Cosmic Medium** composed of protons, electrons, photons, neutrinos, and **Universe-Created Particles** (UCPs), previously referred to as "Dark Matter Particles." This Medium is homogeneous and isotropic, whereas the distribution of Macroobjects (MOs) is spatially inhomogeneous, anisotropic, and temporally non-simultaneous.
  The rejection of the luminiferous aether in 1905 marked a pivotal moment in Classical Physics; however, the Cosmic Medium of WUC may be viewed as a modern, physically grounded revival of this concept—one that restores consistency to Classical Physics rather than undermining it.

Conservation Laws

- **BBM:**
  Does not explicitly address the physical mechanism responsible for the creation of angular momentum, nor does it embed angular momentum conservation as a foundational principle.
- **WUC:**
  Uniquely provides a physical mechanism for the creation of angular momentum and is fully consistent with the fundamental law of its conservation.

Macroobject Formation

- **BBM:**
  Assumes hierarchical formation proceeding *bottom-up*, from extrasolar systems to galaxies and subsequently to superclusters.
- **WUC:**
  Proposes a *top-down* formation scenario, in which superclusters form first and subsequently fragment into galaxies and extrasolar systems (ESS). This process occurs via **Explosive Volcanic Rotational Fission** of overspinning supercluster cores composed of UCPs. These cores were created by the Eternal Universe during the Dark (invisible) Epoch lasting approximately 0.45 Byr. Importantly, the formation of galaxies and ESS is not a completed process of the distant past but is ongoing.

Conclusion

WUC offers a fundamentally different physical picture of the World compared to BBM. It challenges long-

standing assumptions and provides new perspectives on cosmology and Classical Physics. While BBM is primarily mathematical in construction, WUC is grounded in physical mechanisms. Both models may initially appear extraordinary; however, a critical distinction remains: BBM fails to explain a growing body of observational evidence produced by modern astronomy—including results from the *James Webb Space Telescope*—whereas WUC claims natural consistency with these observations.

Ultimately, the validity of any cosmological hypothesis rests on experimental verification. As Richard Feynman famously stated: *"It does not make any difference how beautiful your guess is, it does not make any difference how smart you are, who made the guess, or what his name is. If it disagrees with experiment, it is wrong. That is all there is to it."*

4.4. Latest Discoveries from JWST

The formation of ancient galaxies has long been one of the central problems in cosmology. Based on measurements of CMB, the age of the Universe is estimated to be 13.77 ± 0.06Byr. Astronomers estimate the age of our own MW galaxy to be approximately 13.6 Byr. The Milky Way is one of the two largest spiral galaxies in the Local Group, the other being the Andromeda Galaxy.

Within the framework of BBM, massive, dynamically mature disk galaxies such as MW are not expected to form so early. Their existence therefore places severe constraints on standard galaxy formation scenarios.

Distance Determination and Redshift Measurements

Distances to remote astronomical objects beyond nearby galaxies are inferred primarily through measurements of cosmological redshift. A crucial distinction must be made between **spectroscopic redshifts** and **photometric redshift estimates**. Spectroscopic redshifts, obtained by identifying spectral lines, are conventionally regarded as definitive distance measurements. In contrast, photometric redshifts—derived from broadband photometry—identify *candidate* distant sources and carry significantly larger uncertainties.

JWST High-Redshift Galaxy Discoveries

In our 2024 article *"JWST Discoveries and the Hypersphere World–Universe Model: Transformative New Cosmology"* [1], we discussed galaxies with redshifts $z > 10$. **Tables 3** and **4** present the latest JWST results, adapted from the Wikipedia. (2025) *List of the Most Distant Astronomical Objects*.

Table 3. Most distant galaxies with spectroscopic redshift determinations

Name	Redshift	Years after Big Bang , Mly
MoM-z14	$z = 14.44^{+0.02}_{-0.02}$	280
JADES-GS-z14-0	$z = 14.1796^{+0.0007}_{=0.0007}$	290

Table 4. Notable candidates for most distant galaxies

Name	Redshift	Years after Big Bang , Mly
CEERS U-100588	~32	~100
MIDIS-z25-3	$25.6^{+1.5}_{-1.6}$	

The existence of such galaxies at these epochs—only a few hundred million years after the Big Bang—poses a profound challenge to standard cosmological timelines. According to BBM-based models, there has been insufficient time for the formation, assembly, and dynamical relaxation of massive, rotationally supported disk galaxies with mature stellar populations.

The Growing Cosmological Crisis

As summarized in **Beyond Discovery**:

"Something is very wrong with the universe. We thought we had it figured out—a solid theory that explained everything. And then the James Webb Space Telescope turned on. Almost immediately, it started finding galaxies that break the timeline. Massive, mature galaxies showing up way too early. Like finding a fully grown forest before anyone planted the seeds. That does not work. But the galaxies are there. Okay, so maybe the timeline is off. Except the universe is also expanding at two different speeds depending on how you measure it. And there are structures out there too big to exist. The numbers do not add up. And the more scientists look, the more cracks appear. Something is very wrong. And it keeps getting weirder."

These observations reinforce the conclusion that the current cosmological paradigm is under severe stress. The early emergence of massive, well-organized galaxies, the Hubble tension, and the discovery of extremely large-scale structures collectively suggest that a fundamentally different physical framework—such as that proposed by World–Universe Cosmology—may be required to interpret the data.

4.5. WUC Explanation of the Latest JWST Discoveries

Within the framework of World–Universe Cosmology (WUC), the recent JWST discoveries follow naturally and require no ad hoc modifications to the theory [1]. The key points are summarized below.

1. Cosmological Timing and the Dark Epoch

The apparent paradox posed by extremely early galaxies is fundamentally a question of timing. In WUC, the Beginning of the World occurred **14.22 Byr** ago. The initial **Dark Epoch**, during which only UCM macroobjects existed, lasted approximately **0.45 Byr**. The **Luminous Epoch** began thereafter and has persisted for the past **13.77 Byr**. Consequently, galaxies observed by JWST at very high redshifts formed after the transition to the Luminous Epoch and therefore are not "premature" within WUC temporal framework.

2. Absence of Protogalaxies

Early galaxies emerged in near-present configurations as a direct consequence of the transition from the Dark Epoch to the Luminous Epoch. This transition occurred via **Explosive Volcanic Rotational Fission** of overspinning UCM supercluster cores, accompanied by the **self-annihilation of Universe-Created Particles (UCPs)**. Ordinary matter is a byproduct of this self-annihilation process. As a result, **protogalaxies do not exist in the World**, and therefore JWST does not observe them. This observational absence, which is problematic for Standard Cosmology, is a natural and expected outcome of WUC.

3. Formation of Compact Disk Galaxies

Compact disk galaxies formed through **rotational fission of overspinning UCM supercluster cores**. Each such galaxy contains a single UCM core. Because galaxy formation proceeded through fission rather than hierarchical merging, **frequent early mergers are not expected**. This explains why JWST observes dynamically mature, rotationally supported disk galaxies at extremely high redshifts.

4. Resolution of the Standard Cosmology Paradox

In Standard Cosmology, massive, mature disk galaxies with masses up to

$$M \sim 10^{11}\, M_{\odot}$$

cannot form within the available time span of **100–290 Myr** after the Big Bang, as their assembly is assumed to require several billion years. Such galaxies therefore *should not exist* at the beginning of the Universe. In contrast, WUC predicts their existence and maturity at early epochs, fully consistent with JWST observations.

5. Future Confirmation of Extreme Redshift Candidates

We anticipate that candidate galaxies with extreme redshifts, potentially reaching $z \sim 32$, will be confirmed through future spectroscopic measurements. Their verification depends critically on spectroscopic redshift determination. It is important to emphasize a remarkable implication of WUC: while JWST is now observing the earliest and most distant galaxies, **we ourselves reside in one of the earliest galaxies—the Milky Way**.

This coherence between theory and observation underscores the explanatory power of World–Universe Cosmology in addressing the growing body of JWST data that challenges the foundations of Standard Cosmology.

4.6. Observational Support for WUC from Supernova Cosmology

Strong empirical support for the World–Universe Cosmology (WUC) interpretation emerges from the recent series of papers entitled *"Strong Progenitor Age Bias in Supernova Cosmology"* [17]. These studies demonstrate that the luminosities of Type Ia supernovae (SNe Ia) depend significantly on the age of their progenitor systems, introducing a previously unrecognized and substantial systematic bias into supernova-based cosmology.

Progenitor Age Bias in Type Ia Supernovae

Standard supernova cosmology assumes that the luminosity standardization of SNe Ia is invariant with respect to progenitor age. However, direct measurements of host-galaxy stellar ages reveal a **highly significant correlation** between standardized SN magnitude and progenitor age, detected at the **5.5σ level**. Crucially, this effect is *not* corrected by the commonly used host-galaxy mass-step method.

Once this progenitor age bias is properly accounted for, SNe Ia distance measurements become consistent with **DESI baryon acoustic oscillation (BAO)** results and with **CMB constraints**, eliminating the apparent need for late-time cosmic acceleration.

Implications for Cosmic Expansion

After correcting for progenitor age effects, the combined analysis of SNe Ia, BAO, and CMB data reveals a **greater than 9σ tension** with the standard ΛCDM model. The revised data favor a cosmological scenario in which the expansion of the Universe is **not accelerating at the present epoch** and may instead be decelerating, directly contradicting the ΛCDM interpretation that relies on Dark Energy with a constant equation of state.

As summarized by Junhyuk Son *et al.* [17]:

"Supernova cosmology assumes that the luminosity standardization of Type Ia SNe is invariant with progenitor age. However, direct measurements of host-galaxy ages reveal a highly significant (5.5σ) correlation between standardized SN magnitude and progenitor age. This bias is not corrected by the commonly used mass-step method. After accounting for this effect, SN data align with BAO and CMB results from DESI. Combining SNe, BAO, and CMB reveals a >9σ tension with the ΛCDM model, suggesting a time-varying dark-energy equation of state in a currently non-accelerating universe."

Resolution within World–Universe Cosmology

Within the WUC framework, these results are not indicative of a crisis but rather a natural consequence of applying an **inappropriate constant-H** framework to a Universe in which the expansion rate depends explicitly on cosmological time. WUC predicts that measurements of the Hubble parameter derived from **macroobject-based observations**—such as SNe Ia—will vary due to the spatial inhomogeneity, anisotropy, and temporal non-simultaneity of luminous structures. In contrast, measurements based on the **Cosmic Microwave Background**, which probes the homogeneous and isotropic Cosmic Medium, yield a consistent and physically meaningful value of the expansion rate.

When the Hubble parameter is inferred solely from CMB observations, the so-called **Hubble Tension disappears**, providing strong observational support for WUC and reinforcing its physical interpretation of cosmic expansion.

5. Conclusion

Mainstream cosmology, operating within the framework of the Big Bang Model (BBM), determines the value of the Hubble constant using a diverse set of Macroobject-based indicators. These indicators are drawn from structures whose spatial distribution in the World is intrinsically inhomogeneous, anisotropic, and temporally non-simultaneous, inevitably introducing systematic dispersion into the inferred values of H_0.

In contrast, World-Universe Cosmology (WUC) maintains that the Hubble constant should be determined exclusively from the Cosmic Microwave Background (CMB) Radiation. The CMB reflects the fundamental properties of the Cosmic Medium of the World, which is intrinsically Homogeneous and Isotropic. These properties are largely decoupled from the formation, evolution, and spatial clustering of Macroobjects, whose influence manifests only as secondary perturbations.

From the WUC perspective, the persistent Hubble Tension is therefore not an anomaly requiring ad hoc corrections, but a natural observational signature of the Patchwork Quilt structure of the Visible World. It reflects the inappropriate mixing of local, environment-dependent measurements with a global parameter that characterizes the World as a whole.

Acknowledgments

I express deep gratitude to Academician A. Prokhorov and Prof. A. Manenkov for their pivotal influence on my scientific path. Eternal thanks to my Scientific Father, P. Dirac, whose visionary ideas inspire this work, and to N. Tesla, another extraordinary genius. I extend my sincere thanks to Prof. C. Corda for publishing my manuscripts in the Journal of High Energy Physics, Gravitation and Cosmology. I am also thankful to H. Ricker for valuable comments and suggestions that greatly enhanced the clarity and scope of this model.

References

[1] Netchitailo, V.S. (2024) JWST Discoveries and the Hypersphere World-Universe Model: Transformative New Cosmology. *Journal of High Energy Physics, Gravitation and Cosmology*, **10**, 1806-1834. doi: 10.4236/jhepgc.2024.104102.

[2] Verde, L., Treu, T., and Riess, A. G. (2019) Tensions between the Early and the Late Universe. arXiv:1907.10625.

[3] Wikipedia (2025) Hubble's Law. https://en.wikipedia.org/wiki/Hubble%27s_law.

[4] Mann A. (2019) One Number Shows Something Is Fundamentally Wrong with Our Conception of the Universe. https://www.livescience.com/hubble-constant-discrepancy-explained.html.

[5] Tully, R. B., *et al.* (2014) The Laniakea supercluster of galaxies. Nature, **513**, 71. arXiv:1409.0880.

[6] Gupta, S. (2017) Existence of Many Blue Shifted Galaxies in the Universe by Dynamic Universe Model Came True. *Open Journal of Modelling and Simulation*, **5**, 113-144. doi: 10.4236/ojmsi.2017.51009.

[7] Netchitailo V. S. (2013) Word-Universe Model. viXra:1303.0077v7. https://vixra.org/pdf/1303.0077v7.pdf.

[8] Heymans, C., *et al.* (2008) The Dark Matter Environment of the Abell 901/902 Supercluster: A Weak Lensing Analysis of the HST Stages Survey. Monthly Notices of the Royal Astronomical Society, **385**, 1431-1442.

[9] Zwicky, F. (1933) Die Rotverschiebung von extragalaktischen Nebeln. Helvetica Physica Acta, **6**, 110.

[10] Wang, P., *et al.* (2021) Possible observational evidence that cosmic filaments spin. arXiv:2106.05989.

[11] Boardman, L. (2021) Discovery of a Giant Arc in distant space adds to challenges to basic assumptions about the Universe. https://www.star.uclan.ac.uk/~alopez/aas238_press_release.pdf .

[12] Netchitailo, V. (2023) Dark Stars: Supermassive and Ultramassive Dark Macroobjects. *Journal of High Energy Physics, Gravitation and Cosmology*, **9**, 1021-1043. doi: 10.4236/jhepgc.2023.94075.

[13] Mittal, C. (2023) 5 Most Massive Black Holes Discovered So Far. https://www.secretsofuniverse.in/5-mostmassive-black-holes/.

[14] Netchitailo, V. (2022) Center of Milky Way Galaxy. *Journal of High Energy Physics, Gravitation and Cosmology*, **8**, 657-676. doi: 10.4236/jhepgc.2022.83048.

[15] Haslbauer, M., *et al.* (2022) The High Fraction of Thin Disk Galaxies Continues to Challenge ΛCDM Cosmology. ApJ, **925**, 183. https://iopscience.iop.org/article/10.3847/1538-4357/ac46ac.

[16] NASA Education/Graphics (2021) Hubble Constant H_0 . https://lambda.gsfc.nasa.gov/education/graphic_history/hubb_const.cfm.

[17] Son, J., *et al.* (2025) Strong progenitor age bias in supernova cosmology – II. Alignment with DESI BAO and signs of a non-accelerating universe. Monthly Notices of the Royal Astronomical Society, **544**, 975-987. https://doi.org/10.1093/mnras/staf1685.

Appendix 1. Measurements of the Hubble constant. Adapted from [3].

Date	Hubble const (km/c)/Mpc	Observer	Remarks / methodology
1994	67±7	Supernova 1a Light Curve Shapes	Determined relationship between luminosity of SN 1a's and their Light Curve Shapes. Riess et al. used this ratio of the light curve of SN 1972E and the Cepheid distance to NGC 5253 to determine the constant.
2001-05	72±8	Hubble Space Telescope Key Project	This project established the most precise optical determination, consistent with a measurement of H_0 based upon Sunyaev–Zel'dovich effect observations of many galaxy clusters having a similar accuracy.
2003	72±5	WMAP (First year) only	
2006-08	76.9+10.7 −8.7	Chandra X-ray Observatory	Combined Sunyaev–Zeldovich effect and Chandra X-ray observations of galaxy clusters. Adjusted uncertainty in table from Planck Collaboration 2013.[153]
2007	70.4+1.5 −1.6	WMAP (3 years), combined with other measurements	
2009-02	70.5±1.3	WMAP (5 years), combined with other measurements	
2009-02	71.9+2.6 −2.7	WMAP only (5 years)	
2010	70.4+1.3 −1.4	WMAP (7 years), combined with other measurements	These values arise from fitting a combination of WMAP and other cosmological data to the simplest version of the ΛCDM model. If the data are fit with more general versions, H_0 tends to be smaller and more uncertain: typically around 67±4 (km/s)/Mpc although some models allow values near 63 (km/s)/Mpc.[149]
2010	71.0±2.5	WMAP only (7 years).	
2012-12-20	69.32±0.80	WMAP (9 years), combined with other measurements	
2013-03-21	67.80±0.77	Planck Mission	The ESA Planck Surveyor was launched in May 2009. Over a four-year period, it performed a significantly more detailed investigation of cosmic microwave radiation than earlier investigations

			using HEMT radiometers and bolometer technology to measure the CMB at a smaller scale than WMAP. On 21 March 2013, the European-led research team behind the Planck cosmology probe released the mission's data including a new CMB all-sky map and their determination of the Hubble constant.
2013-10-01	74.4±3.0	Cosmicflows-2	Comparing redshift to other distance methods, including Tully–Fisher, Cepheid variable, and Type Ia supernovae.
2015-02	67.74±0.46	Planck Mission	Results from an analysis of *Planck*'s full mission were made public on 1 December 2014 at a conference in Ferrara, Italy. A full set of papers detailing the mission results were released in February 2015.
2016-05-17	73.24±1.74	Hubble Space Telescope	Type Ia supernova, the uncertainty is expected to go down by a factor of more than two with upcoming Gaia measurements and other improvements. SHoES collaboration.
2016-07-13	$67.6^{+0.7}_{-0.6}$	SDSS-III Baryon Oscillation Spectroscopic Survey (BOSS)	Baryon acoustic oscillations. An extended survey (eBOSS) began in 2014 and is expected to run through 2020. The extended survey is designed to explore the time when the universe was transitioning away from the deceleration effects of gravity from 3 to 8 billion years after the Big Bang.[138]
2016-08-04	$76.2^{+3.4}_{-2.7}$	Cosmicflows-3	Comparing redshift to other distance methods, including Tully–Fisher, Cepheid variable, and Type Ia supernovae. A restrictive estimate from the data implies a more precise value of 75±2.
2016-11-22	$71.9^{+2.4}_{-3.0}$	Hubble Space Telescope	Uses time delays between multiple images of distant variable sources produced by strong gravitational lensing. Collaboration known as H_0 Lenses in COSMOGRAIL's Wellspring (H0LiCOW).
2017-10-16	$70.0^{+12.0}_{-8.0}$	The LIGO Scientific Collaboration and The Virgo Collaboration	Standard siren measurement independent of normal "standard candle" techniques; the gravitational wave analysis of a binary neutron star (BNS) merger GW170817 directly estimated the luminosity distance out to cosmological scales. An estimate of fifty similar detections in the next decade may arbitrate tension of other methodologies.[133] Detection and analysis of a neutron star-black hole merger (NSBH) may provide greater precision than BNS could allow.[134]
2018-02-22	73.45±1.66	Hubble Space Telescope	Parallax measurements of galactic Cepheids for enhanced calibration of the distance ladder; the value suggests a discrepancy with CMB measurements at the 3.7σ level. The uncertainty is expected to be reduced to below 1% with the final release of the Gaia catalog. SHoES collaboration.
2018-04-27	73.52±1.62	Hubble Space Telescope and Gaia	Additional HST photometry of galactic Cepheids with early Gaia parallax measurements. The revised value increases tension with CMB measurements at the 3.8σ level. Continuation of the SHoES collaboration.
2018-07-18	67.66±0.42	Planck Mission	Final Planck 2018 results.
2018-09-05	$72.5^{+2.1}_{-2.3}$	H0LiCOW collaboration	Observations of multiply imaged quasars, independent of the cosmic distance ladder and independent of the cosmic microwave background measurements.
2018-11-06	67.77±1.30	Dark Energy Survey	Supernova measurements using the *inverse distance ladder* method based on baryon acoustic oscillations.
2019-02-08	$67.78^{+0.91}_{-0.87}$	Joseph Ryan et al.	Quasar angular size and baryon acoustic oscillations, assuming a flat ΛCDM model. Alternative models result in different (generally lower) values for the Hubble constant.

2019-03-18	74.03±1.42	Hubble Space Telescope	Precision HST photometry of Cepheids in the Large Magellanic Cloud (LMC) reduce the uncertainty in the distance to the LMC from 2.5% to 1.3%. The revision increases the tension with CMB measurements to the 4.4σ level (P=99.999% for Gaussian errors), raising the discrepancy beyond a plausible level of chance. Continuation of a collaboration known as Supernovae, H_0, for the Equation of State of Dark Energy (SHoES).
2019-03-28	68.0+4.2 −4.1	Fermi-LAT	Gamma ray attenuation due to extragalactic light. Independent of the cosmic distance ladder and the cosmic microwave background.
2019-07-08	70.3+5.3 −5.0	The LIGO Scientific Collaboration, The Virgo Collaboration	Uses radio counterpart of GW170817, combined with earlier gravitational wave (GW) and electromagnetic (EM) data.
2019-07-10	73.3+1.7 −1.8	H0LiCOW collaboration	Updated observations of multiply imaged quasars, now using six quasars, independent of the cosmic distance ladder and independent of the cosmic microwave background measurements.
2019-07-16	69.8±1.9	Hubble Space Telescope	Distances to red giant stars are calculated using the tip of the red-giant branch (TRGB) distance indicator.
2019-08-15	73.5±1.4	M. J. Reid, D. W. Pesce, A. G. Riess	Measuring the distance to Messier 106 using its supermassive black hole, combined with measurements of eclipsing binaries in the Large Magellanic Cloud.
2019-08-20	73.3+1.36 −1.35	K. Dutta et al.	H_0 is obtained analysing low-redshift cosmological data within ΛCDM model. The datasets used are type-Ia supernovae, baryon acoustic oscillations, time-delay measurements using strong-lensing, $H(z)$ measurements using cosmic chronometers and growth measurements from large scale structure observations.
2019-09-12	76.8±2.6	SHARP/H0LiCOW	Modelling three galactically lensed objects and their lenses using ground-based adaptive optics and the Hubble Space Telescope.
2019-10-14	74.2+2.7 −3.0	STRIDES	Modelling the mass distribution & time delay of the lensed quasar DES J0408-5354.
2020-02-26	73.9±3.0	Megamaser Cosmology Project	Geometric distance measurements to Megamaser-hosting galaxies. Independent of distance ladders and cosmic microwave background.
2020-06-18	75.8+5.2 −4.9	T. de Jaeger et al.	Use Type II supernovae as standardisable candles to obtain an independent measurement of the Hubble constant—7 SNe II with host-galaxy distances measured from Cepheid variables or the tip of the red giant branch.
2020-09-29	67.6+4.3 −4.2	S. Mukherjee et al.	Gravitational waves, assuming that the transient ZTF19abanrh found by the Zwicky Transient Facility is the optical counterpart to GW190521. Independent of distance ladders and the cosmic microwave background.
2020-11-07	67.4±1.0	T. Sedgwick et al.	Derived from 88 $0.02 < z < 0.05$ Type Ia supernovae used as standard candle distance indicators. The H_0 estimate is corrected for the effects of peculiar velocities in the supernova environments, as estimated from the galaxy density field. The result assumes $\Omega_m = 0.3$, $\Omega_\Lambda = 0.7$ and a sound horizon of 149.3 Mpc, a value taken from Anderson et al. (2014).[116]
2020-11-25	71.8+3.9 −3.3	P. Denzel et al.	Eight quadruply lensed galaxy systems are used to determine H_0 to a precision of 5%, in agreement with both "early" and "late" universe estimates. Independent of distance ladders and the cosmic microwave background.

2020-12-04	73.5±5.3	E. J. Baxter, B. D. Sherwin	Gravitational lensing in the CMB is used to estimate H_0 without referring to the sound horizon scale, providing an alternative method to analyze the Planck data.
2020-12-15	73.2±1.3	Hubble Space Telescope and Gaia EDR3	Combination of HST photometry and Gaia EDR3 parallaxes for Milky Way Cepheids, reducing the uncertainty in calibration of Cepheid luminosities to 1.0%. Overall uncertainty in the value for H_0 is 1.8%, which is expected to be reduced to 1.3% with a larger sample of type Ia supernovae in galaxies that are known Cepheid hosts. Continuation of a collaboration known as Supernovae, H_0, for the Equation of State of Dark Energy (SHoES).
2020-12-16	72.1±2.0	Hubble Space Telescope and Gaia EDR3	Combining earlier work on red giant stars, using the tip of the red-giant branch (TRGB) distance indicator, with parallax measurements of Omega Centauri from Gaia EDR3.
2021-02	68.7±1.3	Planck+ACTPol+SPTpol_EE 2021	LAMBDA – Resources & Graphics. https://lambda.gsfc.nasa.gov/education/graphic_history/hubb_const.html.
2021-09-17	69.8±1.7	W. Freedman	Tip of the red-giant branch (TRGB) distance indicator (HST+Gaia EDR3)
2021-12-08	73.04±1.04	SH0ES	Cepheids-SN Ia distance ladder (HST+Gaia EDR3+"Pantheon+"). 5σ discrepancy with Planck.
2022-02-08	73.4+0.99 −1.22	Pantheon+	SN Ia distance ladder (+SH0ES)
2022-06-17	75.4+3.8 −3.7	T. de Jaeger et al.	Use Type II supernovae as standardisable candles to obtain an independent measurement of the Hubble constant—13 SNe II with host-galaxy distances measured from Cepheid variables, the tip of the red giant branch, and geometric distance (NGC 4258).
2022-12-14	67.3+10.0 −9.1	S. Contarini et al.	Statistics of cosmic voids using BOSS DR12 data set.[106]
2023-05-11	66.6+4.1 −3.3	P. L. Kelly et al.	Timing delay of gravitationally lensed images of Supernova Refsdal. Independent of cosmic distance ladder or the CMB.
2023-07-13	68.3±1.5	SPT-3G	CMB TT/TE/EE power spectrum. Less than 1σ discrepancy with Planck.
2023-07-19	67.0±3.6	Sneppen et al.	Due to the blackbody spectra of the optical counterpart of neutron-star mergers, these systems provide strongly constraining estimators of cosmic distance.
2024-12-01	72.6±2.0	SH0ES+CCHP JWST	JWST, 3 methods, Cepheids, TRGB, JAGB, 2 groups data
2025-01-14	75.7+8.1 −5.5	Pascale et al.	Timing delay of gravitationally lensed images of Supernova H0pe. Independent of cosmic distance ladder or the CMB. JWST data. (2023-05-11 cell and this one are the only 2 values with this method so far)
2025-05-27	70.39±1.94	W. Freedman et al	Tip of the Red Giant Branch (TRGB) method (values from J-Region Asymptotic Giant Branch (JAGB) and Cepheids also reported)(JWST and HST data)[100]
2025-07	68.76 ± 0.84	WAMP9++2013	LAMBDA – Resources & Graphics. https://lambda.gsfc.nasa.gov/education/graphic_history/hubb_const.html